Advanced Materials Research Vol. 276 (2011) pp 3-19
© (2011) Trans Tech Publications, Switzerland
doi:10.4028/www.scientific.net/AMR.276.3

click for feedback
consult – comment – contact

ZnO films and crystals on bulk silicon and SOI wafers: Formation, Properties and Applications

Eugene Chubenko[1,a], Alexey Klyshko[1,b], Vitaly Bondarenko[1,c], Marco Balucani[2,d], Anatoly Belous[3] and Victor Malyshev[3]

[1]Department of Micro and Nanoelectronics, Belarusian State University of Informatics and Radioelectronics, 220013 P. Brovki str. 6, Minsk, Belarus

[2]Electronic Department, Rome University “La Sapienza”, 00184 via Eudossiana 18, Rome, Italy

[3]Technical Centre “Belmicrosystems”, Integral Corporation, 220064 Kazintsa Sq, Minsk, Belarus

[a]eugene.chubenko@gmail.com, [b]alexi.klyshko@gmail.com, [c]vitaly@bsuir.edu.by, [d]balucani@die.ing.uniroma1.it

Key words: zinc oxide, silicon, porous silicon, electrochemical deposition, hydrothermal deposition

Abstract. In present work the investigation of the electrochemical and chemical hydrothermal deposition processes of ZnO on silicon is presented. The influence of the electrochemical process parameters on the characteristics and morphology of the ZnO deposits is analyzed. Electrochemical deposition from non aqueous DMSO solutions on porous silicon buffer layer is also discussed. The details of the chemical hydrothermal deposition from the nitrate bath of high-quality ZnO crystals on silicon substrate are presented. It was shown that morphology and size of synthesized ZnO crystals depends on the temperature of the deposition bath. Differences between photoluminescence of electrochemically deposited ZnO thin films and hydrothermally synthesized crystals are shown. Electrochemically deposited ZnO films demonstrate defect-caused luminescence and hydrothermally grown ZnO crystals shows intensive exciton luminescence band in UV region. Hydrothermal deposition of high-quality ZnO crystals on the surface of electrochemically deposited ZnO seed layer with porous silicon buffer improves photoluminescence properties of the structure which is useful for optoelectronics applications. Possible applications of ZnO as gas sensors and photovoltaic devices are considered. Aspects of ZnO electrochemical deposition on bulk silicon and silicon-on-isolator wafers for integration purposes are discussed.

Introduction

Zinc oxide is of the considerable attention of researchers due to a series of remarkable semiconductor properties which distinguish it from competing materials such as GaN [1]. Zinc oxide has wider band gap (3.35 eV), low bond energy of excitons (60 meV), and high transmittance in the optical range (90%). These properties together with good piezoelectric and ferromagnetic characteristics define the possibilities for zinc oxide applications in light-emitting devices, photodetectors, solar cells, and sensors [1, 2]. Notable feature of the ZnO is its valuable radiation hardness which is higher than Si, GaAs, CdS and even GaN [3].

A possibility to form the ZnO by a wide variety of techniques used in microelectronics, including such low-cost and easy manufacturing methods as chemical and electrochemical depositions from liquid phase, is a distinguishing feature of this material [4]. By the liquid methods mentioned zinc oxide can be obtained in various structural forms [5, 6]. The basic forms are shown schematically in Fig.1. Hydrothermal method can provide arrays of ZnO crystals from several nanometers to micrometers in size. The potentialities of the electrochemical deposition are more comprehensive. By varying parameters of the electrochemical deposition process (i.e. current density, voltage, reagent concentration, temperature) zinc oxide may be obtained both in the form of single crystals (as in the case of the hydrothermal method) and in the form of continuous polycrystalline and, in certain conditions, epitaxial films [7].

consult
comment
contact
click for feedback

All rights reserved. No part of contents of this paper may be reproduced or transmitted in any form or by any means without the written permission of TTP, www.ttp.net. (ID: 80.94.160.198-10/06/11,09:20:31)

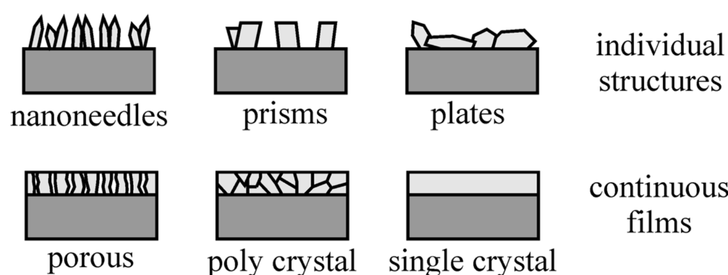

Fig.1. Variety of ZnO morphological structures provided by the electrochemical and hydrothermal methods.

The main advantage of liquid methods for the ZnO production is low outlay for manufacturing equipment and low cost process [7]. The methods are suitable for the fabrication of low-cost photovoltaic devices and sensors. But the electrochemical and hydrothermal methods differ in the application fields that are conditioned by the process features. Films and crystals formed by the electrochemical method contain the structural defects. So, their using as active regions in effective light-emitting devices is not advantageous. However, these films are well suitable as transparent conducting electrode for solar cells, photodetectors, and light-emitting devices. High-temperature oxidation improves properties of the zinc oxide films and expands possible fields of application.

The low process temperature, in most cases below 100°C, is the other advantage of liquid methods. This makes them compatible with the standard microelectronic technology because does not cause a thermal budget to considerable rise and therefore does not increase risk of damage of p-n junctions formed in silicon substrate. The zinc oxide deposition on silicon substrates will allow functional capabilities of silicon ICs to be expanded, new devices of system-on-chip type to be created, and devices based on zinc oxide on the large silicon substrates to be made.

The formation of zinc oxide on silicon is a complicated problem which is typical for heterostructures composed of materials with different lattice parameters and different thermomechanical behavior. To match two semiconductor materials with different structural and thermomechanical properties, i.e. zinc oxide and silicon, buffer layers, for example porous silicon, may be used. Such the method has been used for the formation of films of simple and compound semiconductors on silicon substrates (diamond, GaAs, ZnSe, CdSe, PbS) [8 – 12]. The buffer layer of porous silicon may be covered with metal to protect it against oxidation during the zinc oxide deposition in heated aqueous solutions [13].

This work discusses the formation of various morphological forms of zinc oxide on silicon substrates by liquid electrochemical and hydrothermal methods for numerous applications.

Hydrothermal synthesis of ZnO crystals

The hydrothermal deposition technique is a simple method for the formation of arrays of zinc oxide crystals on any substrate, including dielectric one, of any area. Crystals obtained by this technique are noted for the high crystal perfection. This is one of the factors that allow manufacturing not only arrays of nanocrystals but ingots of large diameter for the ZnO substrate production as well. This work discusses the hydrothermal deposition of arrays of zinc oxide crystals on silicon substrates with the pretreated surface.

The hydrothermal synthesis of ZnO crystals was carried out on the n^+-type antimony doped Si (111) wafers of 0.01 Ohm·cm resistivity by the one-step process. The 0.1 M equimolar aqueous solution of zinc nitride and $Zn(NO_3)_2$ and hexamethylenetetramine $C_6H_{12}N_4$ was used. To maintain the pH of the solution equal to 5, some extra quantity of ZnO was added to the solution [14]. $C_6H_{12}N_4$ was added just prior to the experiments. The reaction chamber volume was 20 ml. The thermo control unit was used to maintain the chamber at the selected constant temperature.

Silicon substrates before the experiments were treated for 10 min in the 4.5% HF to remove natural oxide. Substrates were immersed in the solution and then the reaction chamber was heated up to the target temperature and kept at that temperature for certain time (2 h). After the deposition of ZnO the samples were rinsed in deionized water and dried [15, 16].

click for feedback
consult – comment – contact
consult comment contact
click for feedback

Fig. 2 shows scanning electron microscopy SEM images of the ZnO nanocrystals formed at various temperatures. SEM images were obtained with Hitachi S-4800 (Japan) scanning electron microscope operating at 15 kV. As seen in Fig.2, ZnO columns are of the strictly hexahedral shape characteristic of crystals with hexagonal lattice. It is unusual that ZnO crystals formed at the temperature of 75ºC have the pronounced twin structure. This effect is not observed for higher temperatures of the reacting medium. Factors responsible for the formation of such the structure remain to be investigated.

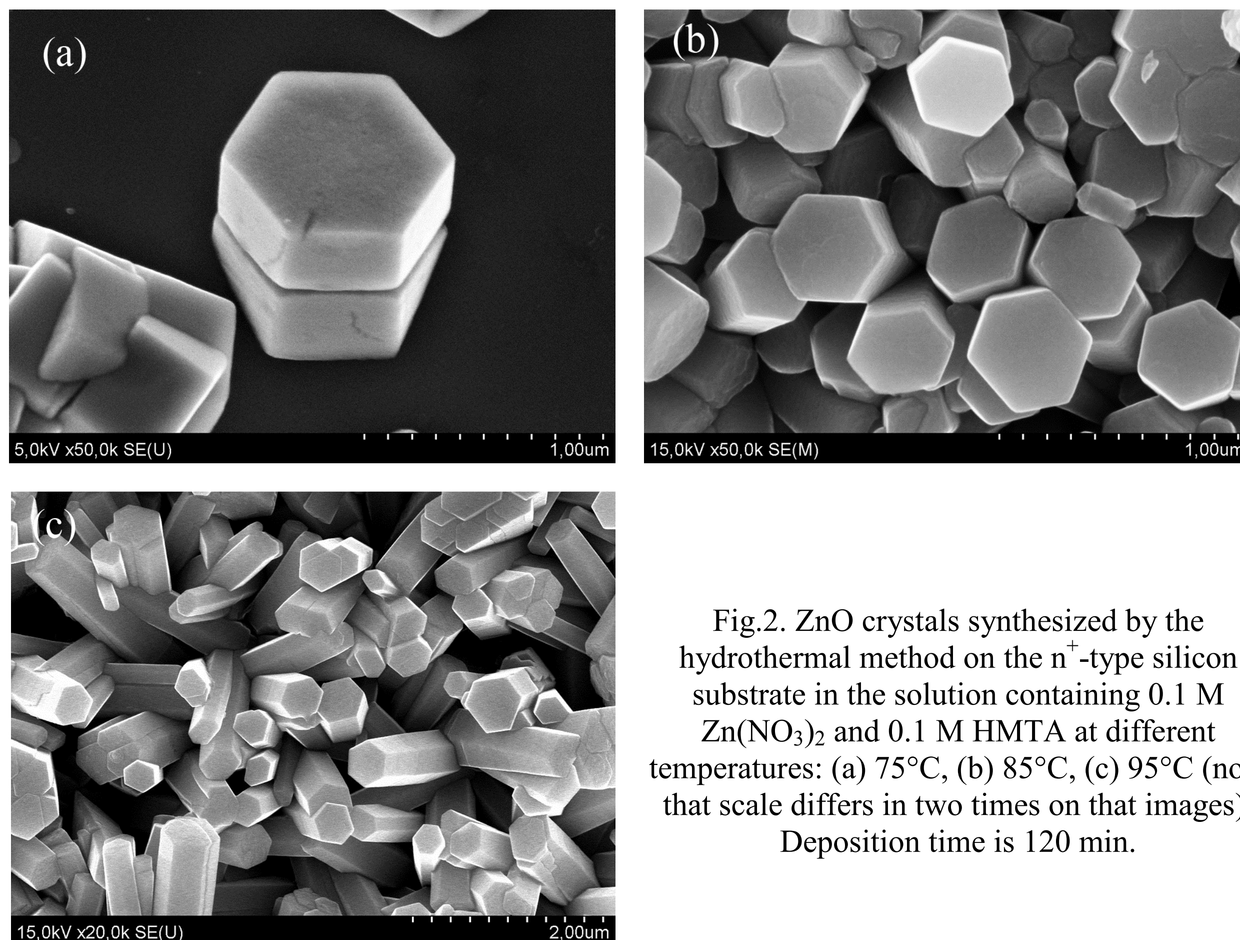

Fig.2. ZnO crystals synthesized by the hydrothermal method on the n^+-type silicon substrate in the solution containing 0.1 M $Zn(NO_3)_2$ and 0.1 M HMTA at different temperatures: (a) 75°C, (b) 85°C, (c) 95°C (note that scale differs in two times on that images). Deposition time is 120 min.

The crystal size and compactness of crystal arrangement on the substrate depend on the synthesis temperature. For the same deposition times, the increase in the temperature of the reacting medium causes the decrease of the crystal diameter and increase in the crystal height, resulting from the increase of the formation rate of crystals. For the temperature of the reacting medium of 75ºC, the crystal diameter is 800 nm. For the temperatures of 85ºC and 95°C, the diameters of zinc oxide crystals synthesized are 600 and 500 nm, correspondingly. The number of crystals on the substrate surface increases with temperature. This can be conditioned by the activation of greater number of crystal nucleation sites when the heat energy of the system increases.

Thus, the hydrothermal deposition technique allows arrays of zinc oxide crystals of various sizes to be formed. Crystal sizes are controlled by the temperature of the reacting medium.

Electrochemical deposition of ZnO

Electrochemical deposition of ZnO from aqueous solution on buffer layer. The most common electrochemical ZnO deposition bath is based on the zinc nitride salt $Zn(NO_3)_2$. It is agreed that the electrochemical deposition of zinc oxide from such kind of solution could be considered as a two stage process [17]:

click for feedback consult - comment - contact

$$Zn(NO_3)_2 + 2H_2O + 2e^- \rightarrow Zn^{2+} + 2NO_2^- + 4OH^- \;(-0.189 \text{ V vs. Ag/AgCl}) \quad (1)$$

$$Zn^{2+} + 2OH^- \rightarrow Zn(OH)_2 \rightarrow ZnO + H_2O \quad (2)$$

At the first stage, the ions of acid residue of nitric acid with the participation of electrons transform into the ions of acid residue of nitrous acid with the formation of the hydroxyl ions (reaction 1). An accumulation of a great quantity of the hydroxyl ions results in the local increase of pH at the cathode space. In alkaline solutions, the presence of the zinc hydroxide phase is possible which can decompose spontaneously with the ZnO formation (reaction 2). As follows from the above expressions, the process of the ZnO electrochemical deposition should take place at the potentials close to zero, however ZnO deposition is observed only at the potentials below – 0.7 V. A small value of the reaction rate constant and low diffusion rates of reagents result in a considerable overvoltage of the deposition of the semiconductor compound [18]. Moreover, to deposit ions of acid residue of nitric acid, adsorbed Zn^{2+} cations acting as the process catalyst are required on the cathode surface. For this reason, the ZnO deposition potential shifts to the range of the Zn deposition potentials.

Fig. 3 shows two cycles of the cyclic voltammograms of the Ni electrode in the aqueous solution containing 0.1 M $Zn(NO_3)_2$ at 60°C. Voltammetric investigations were carried out in a three-electrode glass electrochemical cell equipped with a magnetic stirrer and a temperature control unit. The standard commercial Ag/AgCl electrode served as the reference electrode. The counter electrode was a platinum wire. It should be noted that the first cycle considerably differs from the second cycle and, as we have determined experimentally, from the subsequent ones.

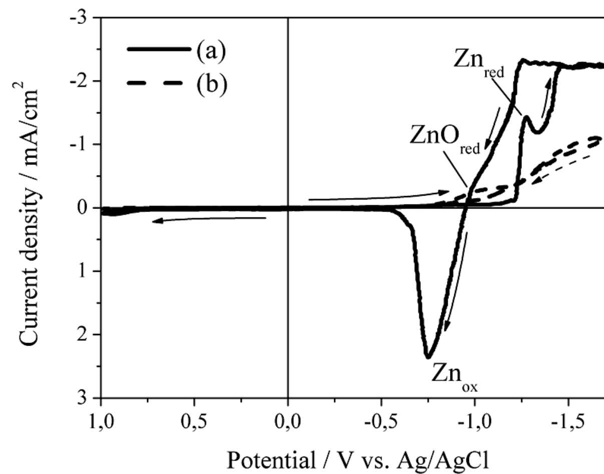

Fig.3. Cyclic voltammograms of the Ni electrode in the aqueous solution containing 0.1 M $Zn(NO_3)_2$ at 60°C: (a) first scan, (b) second scan. Scan rate is 100 mV/s.

For the first scan, the pronounced current density peak at the cathode polarization in the range of – 1.3 V corresponds to the metallic zinc deposition by the reaction, the standard potential of which relative to the Ag/AgCl reference electrode is – 0.958 V:

$$Zn^{2+} + 2e^- \rightarrow Zn \quad (3)$$

The shift of the potential of this reaction may be conditioned by the overvoltage and imperfect electrode surface. At the anode polarization around – 0.8 V, the current peak associated with the dissolution of metal deposited at the cathode polarization is observed. The current increase at the potentials above – 1.3 V is conditioned by the hydrogen evolving at the cathode due to the direct water electrolysis. A plateau observed in Fig.3 in this range is associated with current limiting by the potentiostat not with the processes in the electrochemical cell.

click for feedback
consult – comment – contact
consult comment contact click for feedback

Behavior of the current during second and all subsequent potential scans was the same. The current peak in the range from – 0.9 V to – 1.1 V was observed in the curves at the cathode polarization. Similar behavior of the current in the cyclic voltammograms is characteristic for the deposition of other metal chalcogenides from aqueous electrolytes [11]. So, this range should correspond to the deposition of the ZnO binary compound via the Zn^{2+} ions absorbed at the cathode surface [17].

The cyclic voltammogram technique allowed us to determine parameters required for the zinc oxide deposition on the nickel substrates in the potentiostatic regime. However, from the practical point of view, it is advantageous to use the galvanostatic regime. To switch to the galvanostatic regime, the densities of current flowing through the electrochemical system during the zinc oxide deposition in the potentiostatic regime were determined. These were in the range of 2 – 10 mA/cm^2.

For the electrochemical deposition of ZnO from the aqueous solution n^+-type antimony doped Si (111) substrates (0.01 Ohm·cm) covered with the electrochemically deposited Ni layer were prepared. Prior to the Ni deposition Si substrates were immersed in the 4.5% HF solution to remove the native oxide layer. After that they were treated in the HF solution ($HF:H_2O:C_3H_7OH$ = 1:3:1) for 15 s under the anode polarization at the current density 70 mA/cm^2. Fabricated at this stage the thin mesoporous silicon layer (0.8 µm) increases adhesion and reduces mechanical strains of metal and semiconductor films deposited on it. The Ni layer was electrochemically deposited from the commercial sulfamic solution. The thickness of the Ni layer was 100 nm.

Fig.4 demonstrates SEM images of the ZnO films electrochemically deposited on the silicon substrates with the nickel buffer layer in the galvanostatic regime from the aqueous 0.1 M $Zn(NO_3)_2$ solution (pH = 5) at the 70°C electrolyte temperature and at the current densities from 2.5 to 7 mA/cm^2. The thickness of the ZnO films formed at different current densities was kept constant and equal to 6 µm. This was achieved by controlling the deposition time. The films are of good adhesion to the substrate surface and of high mechanical strength.

Referring to Fig.4, the structure of the ZnO films formed is obvious to depend on the deposition current density. As the current density increases, the deposit becomes more compact. So, for the 2.5 mA/cm^2 current density, the deposit is the porous film, and for the 7 mA/cm^2 current density, it is a continuous film with the smooth surface and substantially smaller number of structural defects.

The study of the elemental composition by the X-ray microanalysis revealed that the zinc oxide deposit always contains of 50 atomic percents of zinc and 50 atomic percents of oxygen, i.e. it is of stoichiometric composition. The study of the phase constitution by the X-ray diffractometry method (XRD) carried out on DRON-3 apparatus (RPE "Bourevestnik" Inc., Russia) using the CuKα source revealed that the zinc oxide films consist of the ZnO crystals with the preferred orientation (0002) as seen in Fig.5. The sample formed at the 5 mA/cm^2 current density demonstrates a maximum response related to this phase.

Fig. 6 shows XRD spectra of the same ZnO films after the thermal treatment at 500°C in air. As seen from Fig.6, the thermal treatment resulted in the little increase of peaks associated with the (0002) ZnO phase. This can be related to the partial recrystallization of amorphous zinc oxide existing in small proportion in deposit.

So, technological regimes discussed allow forming polycrystalline structured zinc oxide films with various morphologies (from porous to compact) on the silicon substrates with buffer layer.

Electrochemical deposition of ZnO on porous silicon from non-aqueous solution. In contrast to heated aqueous electrolytes, in the non-aqueous solutions based on DMSO the oxidation and rupture of porous silicon do not take place [18]. Moreover, the parasitic deposition of zinc hydroxide cannot occur in the non-aqueous solutions based on DMSO. In addition, to improve crystalline quality of deposit, such the solution may be heated up to the temperature above 100°C because DMSO boiling point is equal to 189°C [19].

click for feedback
consult – comment – contact
consult comment contact click for feedback

click for feedback
consult – comment – contact

Fig. 7 shows cyclic voltammograms of the PS electrode obtained in the non-aqueous DMSO solution containing various concentrations of zinc chloride (0.03 M and 0.06 M $ZnCl_2$) at 80°C. A change in the concentration of zinc ions resulted only in an intensification of the dissolution peak in the anodic branch of the voltammogram in the range of 0.2 V, suggesting that this peak is related with the oxidation of zinc ions. At the cathode polarization, only a current plateau in the range from – 1.8 V to – 2.4 V is observed to be associated with the zinc oxide deposition.

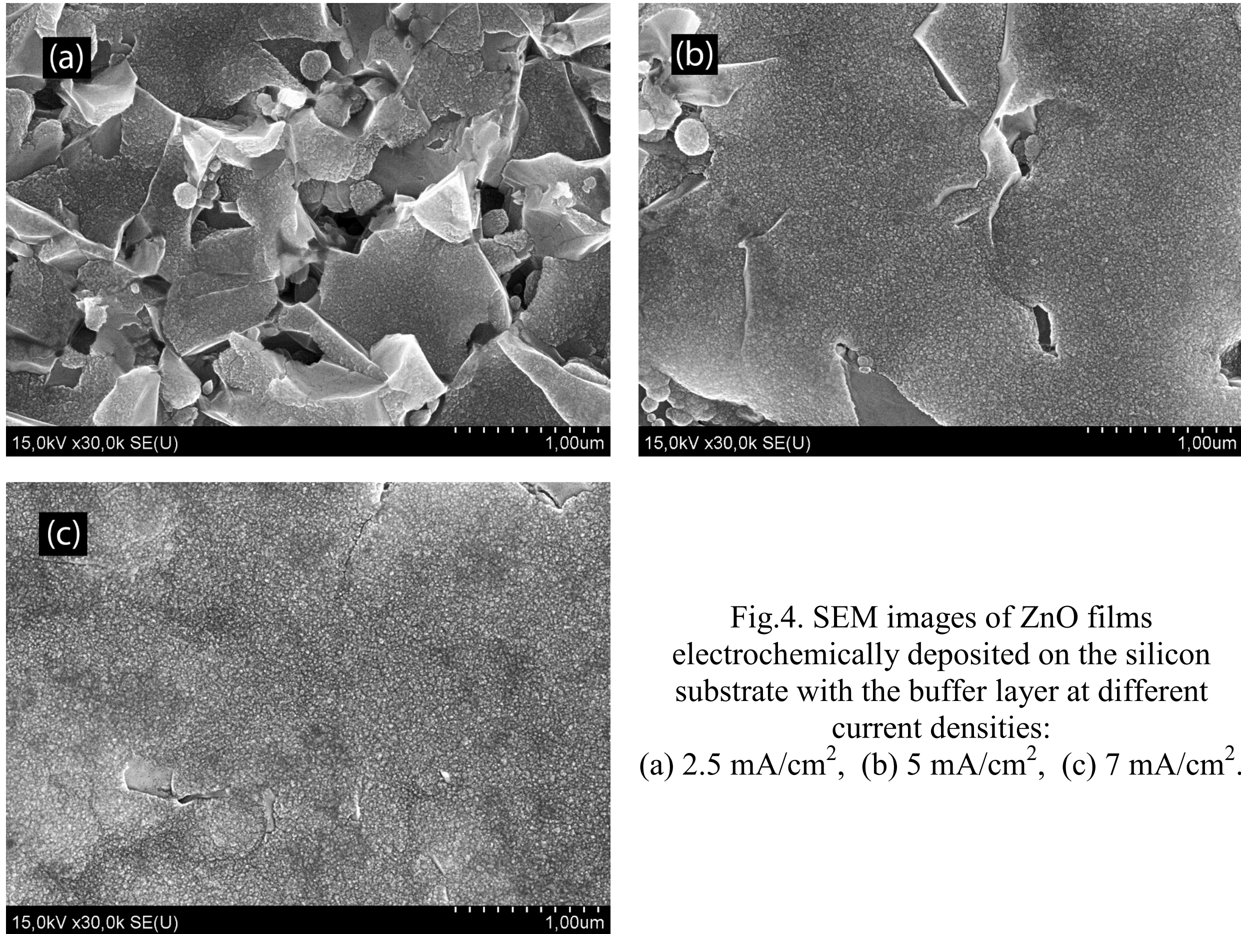

Fig.4. SEM images of ZnO films electrochemically deposited on the silicon substrate with the buffer layer at different current densities:
(a) 2.5 mA/cm^2, (b) 5 mA/cm^2, (c) 7 mA/cm^2.

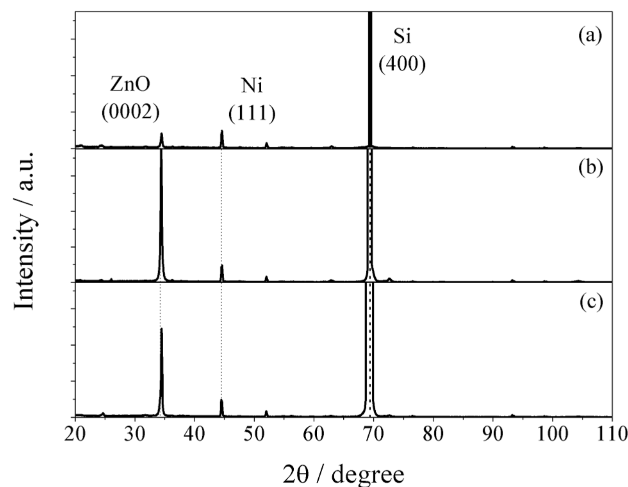

Fig.5. XRD spectra of ZnO films electrochemically deposited on the silicon substrate with the buffer layer at different current densities: (a) 2.5 mA/cm^2, (b) 5 mA/cm^2, (c) 7 mA/cm^2.

consult
comment
contact
click for feedback

click for feedback
consult – comment – contact

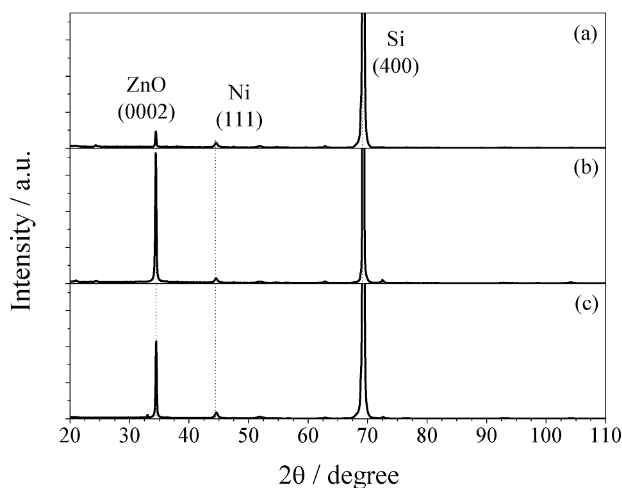

Fig.6. XRD spectra of ZnO films electrochemically deposited on the silicon substrate with the buffer layer at different current densities: (a) 2.5 mA/cm^2, (b) 5 mA/cm^2, (c) 7 mA/cm^2, after thermal treatment at 500°C in air.

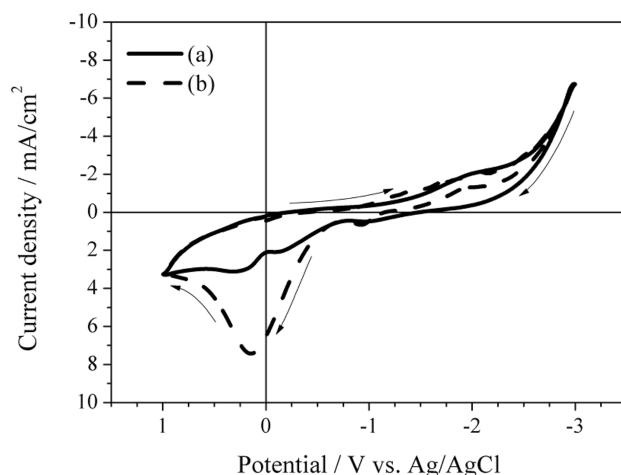

Fig. 7. Cyclic voltammograms of the PS electrode in the non-aqueous DMSO solution containing: (a) 0.03 M $ZnCl_2$ + 0.1 M KCl and (b) 0.06 M $ZnCl_2$ + 0.1 M KCl at 80°C. The scan rate is 1 V/s.

The formation of zinc oxide from non-aqueous solutions was also made in the galvanostatic regime. For that the range of the current densities for the ZnO deposition in the potentiostatic regime was specified to be from 0.1 to 5 mA/cm^2.

Fig. 8 demonstrates SEM micrographs of the top surface and cross section of the zinc oxide film deposited on the silicon substrate with the buffer porous silicon layer from the 0.03 M $ZnCl_2$+0.1 M KCl solution at the 95°C temperature and 0.5 mA/cm^2 current density. As seen from Fig.8, the zinc oxide deposition takes place not only on the surface, but inside the porous layer as well. It was noticed that deposition process at an initial stages take place inside the pores of porous silicon. This is clearly demonstrated by SEM micrographs. For the 25 min deposition time, zinc oxide crystals are practically absent at the sample surface Fig. 8 (a), but single crystals are well observed on the pore sidewalls Fig. 8 (b). When the deposition time was increased up to 45 min, a polycrystalline zinc oxide film was formed at the porous silicon surface Fig. 8 (c), and the pore sidewalls were covered with the continuous zinc oxide layer Fig. 8 (d).

It was supposed that the electroconductivity of the electrolyte columns inside pores exceeds electroconductivity of the silicon skeleton of porous silicon, allowing ZnO to deposit first on the pore walls, and then at the surface of the PS layer. Otherwise material deposition only takes place on top of the structure. That statement was confirmed by the series of the experiments of a ZnO

consult
comment
contact
click for feedback

click for feedback consult - comment - contact

electrochemical deposition on silicon substrates with a porous silicon buffer layer of different thickness. Three samples marked as (I), (II), and (III). The thicknesses of the porous silicon layers were 1 μm for the sample (I), 3 μm for the sample (II), and 6 μm for the sample (III). These thicknesses were provided by the anodization of the silicon wafers in the $HF:H_2O:C_3H_7OH = 1:3:1$

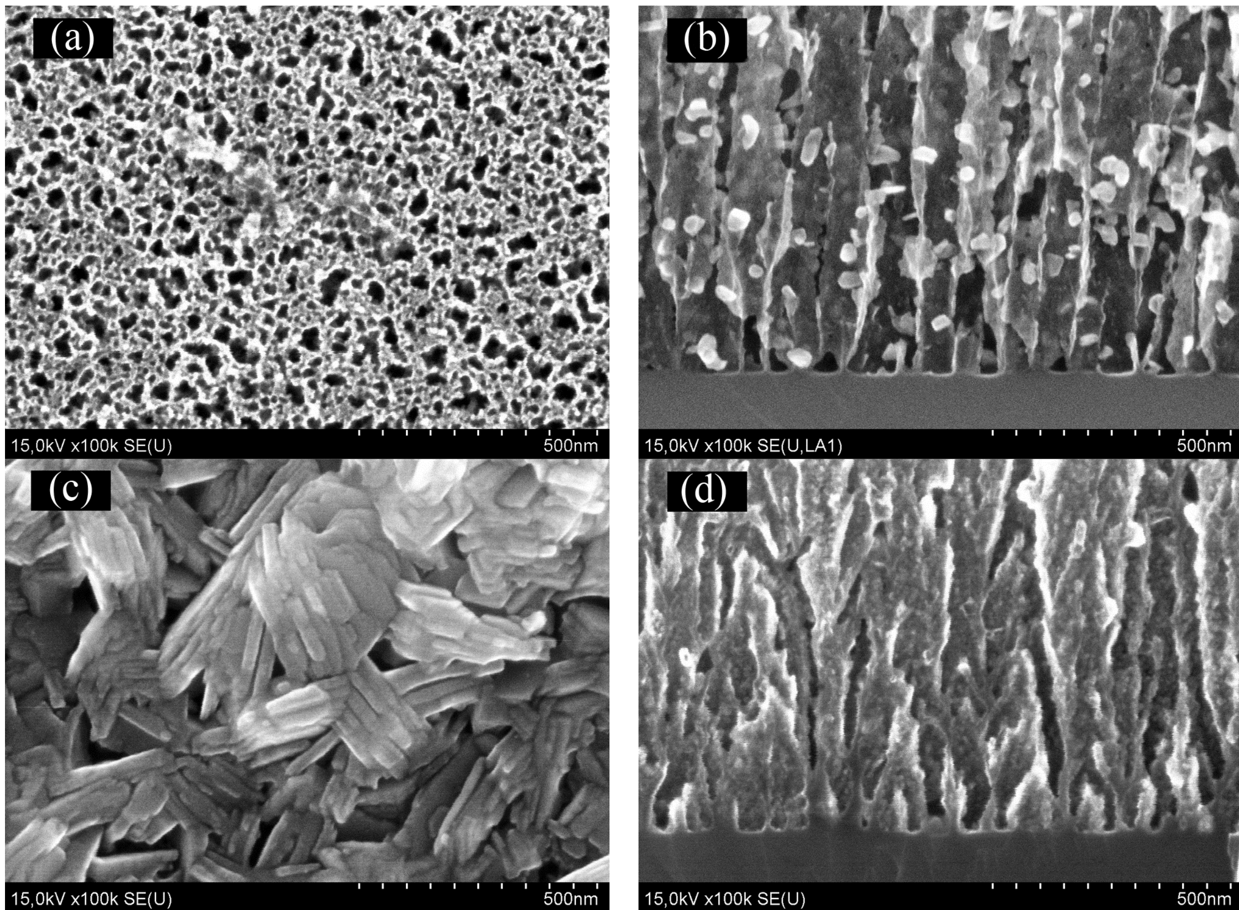

Fig.8. Plan views and cross sections views of ZnO crystals deposited on the n^+-type silicon substrate with the buffer porous silicon layer from the DMSO based solution containing 0.03 M $ZnCl_2$ and 0.1 M KCl for different deposition times: (a, b) 25 min, (c, d) 45 min.

solution at the current density 70 mA/cm^2 for 20 sec, 1 min, and 2 min correspondingly. The porosity of the formed porous silicon was 70%, pore diameter was less than 50 nm.

Fig.9 shows cross sections and plane views of the described above samples.

Figs. 9 (a) and (b) correspond to sample (I). The thickness of this zinc oxide layer on sample (I) is of 480 nm, the layer surface is rough, and the layer consists of small grains. Zinc oxide penetrates into the pore channels of porous silicon to the depth not higher than 100 nm. As seen on Fig. 9 (b) zinc oxide layer deposited on the surface seems to be continuous. As for the surface analysis of the sample (I), the zinc oxide layer consists of the round aggregates mainly 150 – 300 nm. The SEM photograph also shows that aggregates discussed in turn consist of a great number of particles only a few nanometers in size. Figs. 9 (c) and (d) correspond to sample (II). As may be seen in Fig. 9 (c), the zinc oxide layer is observed at the PS surface. The thickness of this layer is about 200 nm to be less in comparison with the 480 nm thick zinc oxide layer deposited on the surface of the sample (I) at the same conditions. This is indirectly testifies that the pores in sample (II) were filled with zinc oxide much deeper. In addition to the difference in the thicknesses of the surface zinc oxide layers, sample (II) is characterized by much deeper filling of pore channels with zinc oxide and substantially more material at porous silicon layer at all. Referring to Fig. 9 (d), the analysis of the SEM images of the sample (II) surface shows that the zinc oxide layer deposited on the surface consists of the round aggregates 200 – 400 nm in diameter as is the surface layer of the sample (I).

consult comment contact click for feedback

As compared with the sample (I), the sample (II) demonstrates more uniform zinc oxide layer containing less large aggregates. Figs. 9 (e) and (f) show SEM images of the sample (III) correspondingly. Zinc oxide film thickness on the surface varied across the surface. In some areas it is almost absent, as seen on Fig 9 (e). It is significant that zinc oxide penetrates the whole thickness of the 6 μm thick porous silicon layer. Zinc oxide inside pores looks like homogeneous glass-like

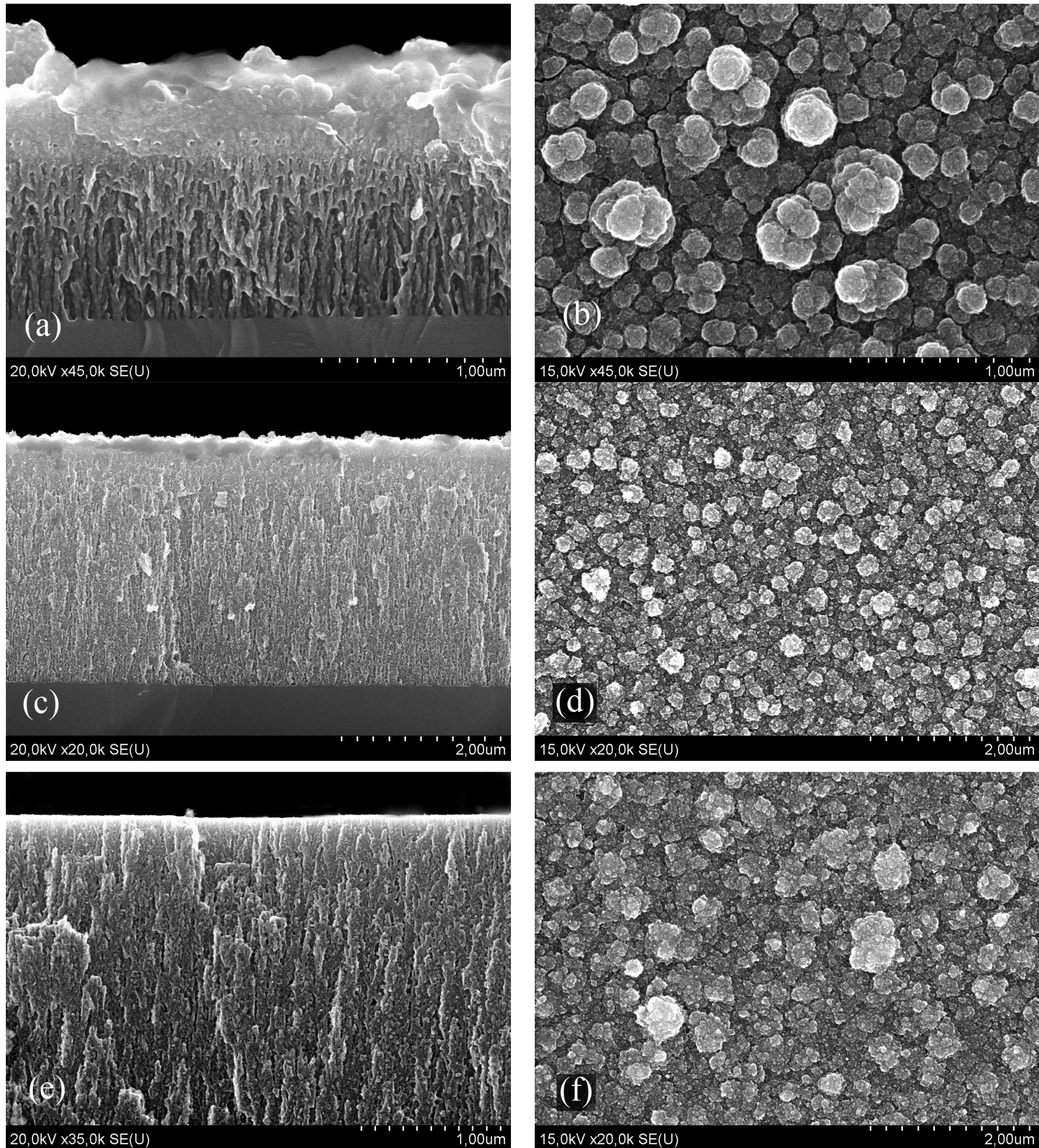

Fig.9. SEM images of the samples after ZnO deposition from DMSO solution representing sample (I): (a) cross-section and (b) plan view; sample (II): (c) cross-section and (d) plan view; sample (III): (e) cross-section and (f) plan view.

material. The pore channels are filled with zinc oxide not completely. The structure of the pore channels characteristic of the initial mesoporous silicon is observed in the sample (III) despite of pore filling with zinc oxide. The analysis of the SEM plan view images showed that the surface zinc oxide layer consists of the aggregates constituted by zinc oxide particles as in case of sample (II).

click for feedback
consult – comment – contact

click for feedback
consult – comment – contact

The results of the experiments show that zinc oxide can be deposited on the substrates with the porous silicon buffer layer from non-aqueous electrolytes based on DMSO and zinc chloride.

The results of the experiments show that the non-aqueous DMSO based solution allows the zinc oxide to be deposited directly on the buffer porous silicon layer. In this case the thickness of the porous silicon layer, i.e. the height of silicon crystallites making up the skeleton of porous silicon, is of considerable importance in the pore filling with zinc oxide. The effective pore filling for the PS type used was achieved only with the PS layer thickness no less than 5 µm. If zinc oxide penetrates into the depth of the porous silicon matrix, its adhesion to the substrate surface increases as well as the contact area between both materials. It is very important in the integration of such different in stress-strain properties materials as zinc oxide and silicon.

Hydrothermal deposition of ZnO on electrochemically deposited ZnO seed layer. As ZnO crystals obtained by the hydrothermal technique are noted for their high structural perfection and good luminescence properties it is purposeful to deposit ZnO crystals on the surfaces of electrochemically deposited ZnO layer formed on the buffer porous silicon layer to provide its ultraviolet luminescence characteristics. For the experiments same samples (I) – (III) were used.

Fig. 10 (a) shows plan view SEM image of the sample (I) after the hydrothermal treatment. It is evident that the film consisted of hexahedral crystals characteristic of zinc oxide crystals having the hexagonal lattice was formed on the sample surface. The film surface is highly developed and contains a lot of structural defects. The SEM image of the sample cross-section shown in Fig.10 (b) indicates that the film in the depth of the porous silicon layer again consists of random crystals succeeded to the surface morphology of the oxide zinc electrochemically deposited. The thickness of the hydrothermal ZnO layer is 500 nm. The clear interface between the electrochemical and hydrothermal layers of zinc oxide is not observed. Noteworthy also is the smooth zinc oxide/porous silicon junction without a sharp boundary and cross cracks. Fig.10 (c) demonstrates plan view of the sample (II) after the hydrothermal treatment. In contrast to the sample (I), zinc oxide film on the surface of the sample (II) consists of grown together hexahedral crystals with well-defined faces. The size of single crystals is 100 – 300 nm. The SEM image of the sample cross-section shown in Fig.10 (c) displays that crystals of the hydrothermal zinc oxide are all-of-a-piece as distinct from the sample (I) and grow directly on the electrochemical zinc oxide layer. The layer thickness is also about 500 nm. Fig.10 (e) and (f) shows plan view and cross-section images of the sample (III). Situation for the sample (III) is similar to the sample (II), however the crystals are larger in size and they separated from one another more distinctly. Crystals are up to 600 nm in diameter. They settle at a big angle to the sample surface that relates to the developed surface morphology of the initial substrate.

So, it may be concluded that the size and arrangement of zinc oxide crystals deposited by the hydrothermal method considerably depend on the surface morphology of the initial substrate, i.e. the surface of the zinc oxide film electrochemically deposited, which in turn is conditioned by the characteristics of the buffer porous silicon layer. We suppose that highly grain-oriented polycrystalline and single-crystal zinc oxide film may be provided by fitting parameters of the porous silicon layer.

Photoluminescence properties of ZnO formed by electrochemical and hydrothermal techniques

Photoluminescence of semiconductor material is a powerful tool to obtain information about the structure of its energy band and crystal perfection. Photoluminescence spectra show a presence of impurities and lattice defects that result in the formation of impurity levels in the band gap, which, in turn, decrease intensity of exciton luminescence bands and give new proper luminescence bands. The photoluminescence spectra of ZnO were measured by the SOLAR MS 7504i monochromator (SOLAR TII, Belarus) with the Xe lamp (1000 W) as an excitation light source and the Hamamatsu S7031 (Japan) FFT-CCD image sensor as a detector. To cut out monochromatic lines from wide spectrum of the Xe lamp, SOLAR DM 160 monochromator was used. All measurements were carried out at room temperature.

consult comment contact click for feedback

click for feedback
consult – comment – contact

Fig. 11 shows the photoluminescence spectra of the zinc oxide films electrochemically deposited from the aqueous solution on the silicon substrates with the nickel buffer layer. As seen from Fig. 11, the zinc oxide films demonstrate only one wide photoluminescence band with

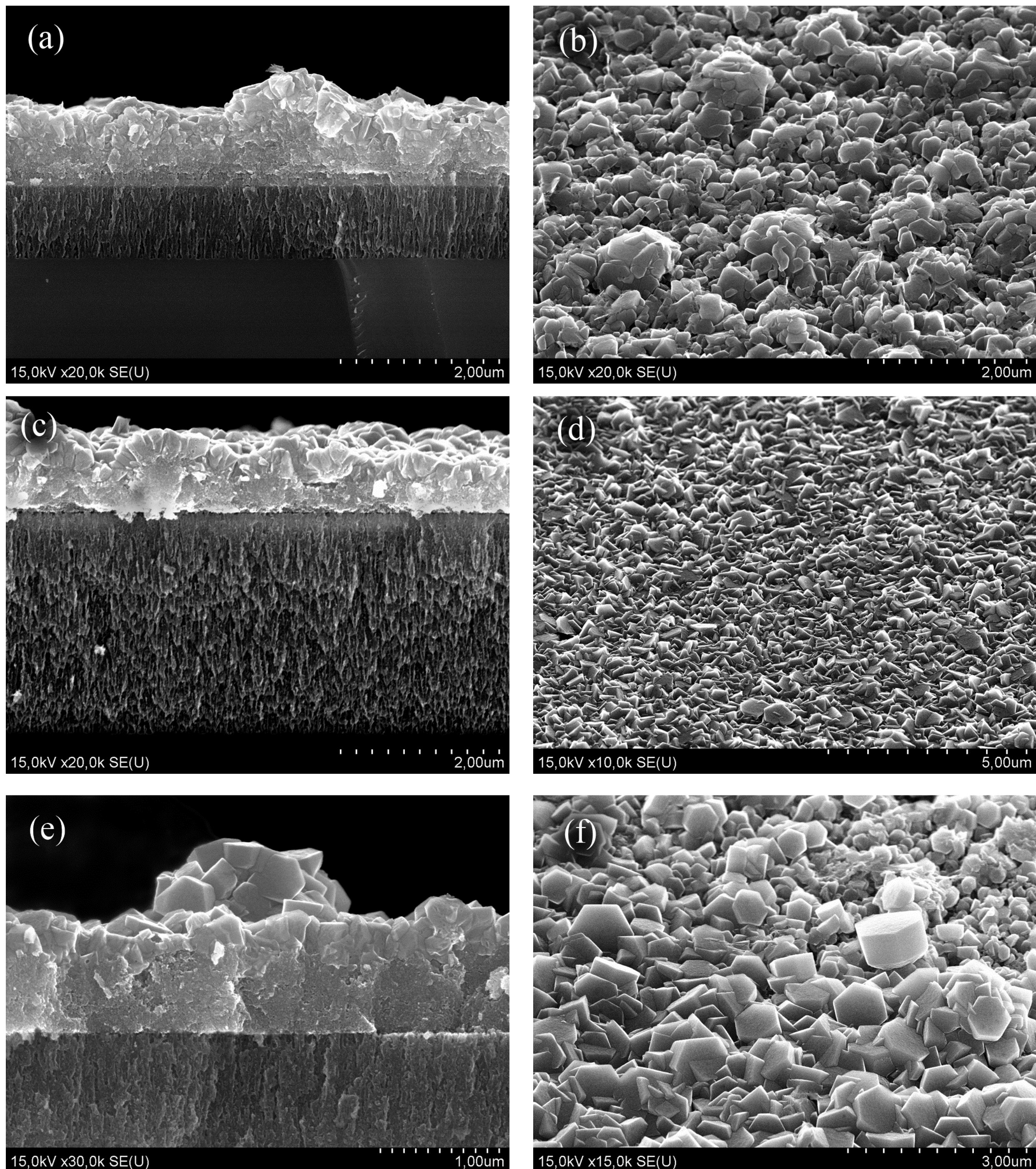

Fig.10. SEM images of the samples after hydrothermal ZnO synthesis on electrochemically formed ZnO seed layers representing sample (I): (a) cross-section and (b) plan view; sample (II): (c) cross-section and (d) plan view; sample (III): (e) cross-section and (f) plan view

maximum at near 610 nm in the red-orange range of the electromagnetic radiation spectrum. As the samples under study were not doped specially and were free from unintentional impurities, it is obvious that this band is conditioned by internal defects of material. A thermal annealing in air at the temperature of 500ºC results in the decrease in the intensity and shift of the photoluminescence maximum to the more long-wave range to the wavelength 680 nm as demonstrated in Fig. 12.

consult
comment
contact
click for feedback

click for feedback
consult – comment – contact

The photoluminescence band observed may consist of two independent bands conditioned by the recombination processes via the levels in the semiconductor band gap due to ionized oxygen vacancies and oxygen atoms in the interstitial sites of the ZnO crystal lattice [20]. The photoluminescence band emitted by the oxygen vacancies has maximum in the more short-wave

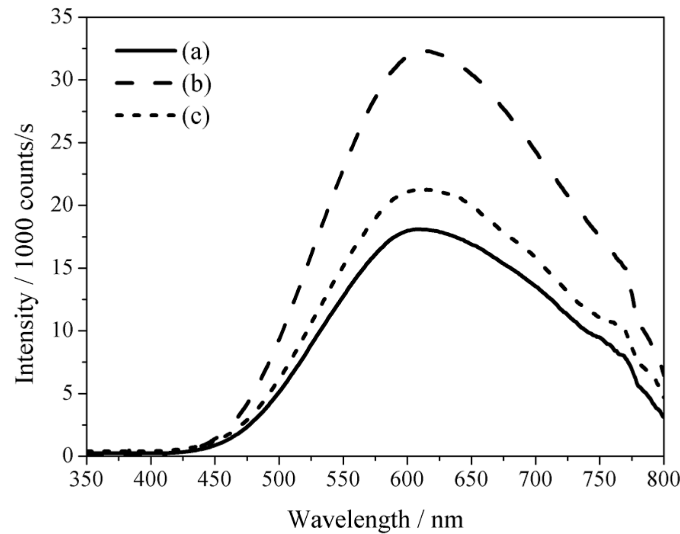

Fig.11. Photoluminescence spectra of ZnO thin films deposited on the silicon substrate with the buffer Ni layer at different current densities: (a) 2.5 mA/cm^2, (b) 5 mA/cm^2, (c) 7 mA/cm^2.

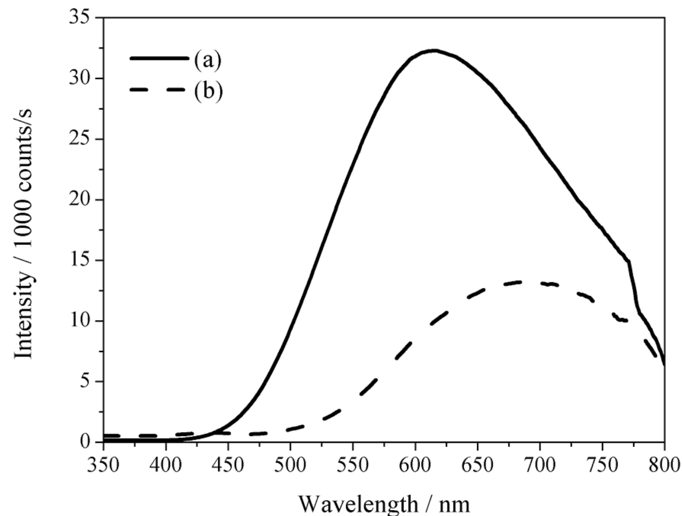

Fig.12. Photoluminescence spectra of ZnO thin films deposited on the silicon substrate with buffer Ni layer at the current density 5 mA/cm^2 (a) before and (b) after the thermal treatment at 500°C for 15 min in air.

(550 nm) range of the spectrum, while the band emitted by the oxygen atoms in the interstitial sites has maximum at longer (650 nm) wavelength. The position and intensity of maxima can vary depending on wavelength of the exciting radiation [20] and material structure [20, 21].

When the ZnO film is annealed in air, free oxygen is adsorb by the material surface, ionized, and embedded in the ZnO crystal lattice. Hence, the most part of the oxygen vacancies is compensated, while the concentration of the oxygen atoms in the interstitial sites remains the same and even increases at the surface. These processes result in the decrease in the intensity of the photoluminescence band (at 550 nm) associated with the ionized oxygen vacancies. The intensity of the photoluminescence band conditioned by the oxygen atoms in the interstitial sites of the ZnO crystal lattice remains the same at that or may slightly increase [20].

consult
comment
contact
click for feedback

Fig.13 shows the photoluminescence spectrum of the ZnO thin film deposited on the silicon substrate with the buffer porous silicon layer from the DMSO solution before and after treatment in hydrothermal ZnO deposition bath. Before treatment only one wide photoluminescence band with maximum at 575 nm in the yellow-green range is observed in the figure. The shift of this band maximum to the short-wave range of the electromagnetic spectrum indicates that in this case defect photoluminescence is conditioned by oxygen vacancies. And after treatment also narrow band in the UV region appeared. This wavelength corresponds to the band gap energy of perfect ZnO crystals (3.35 eV) and is emitted due to the recombination of free excitons.

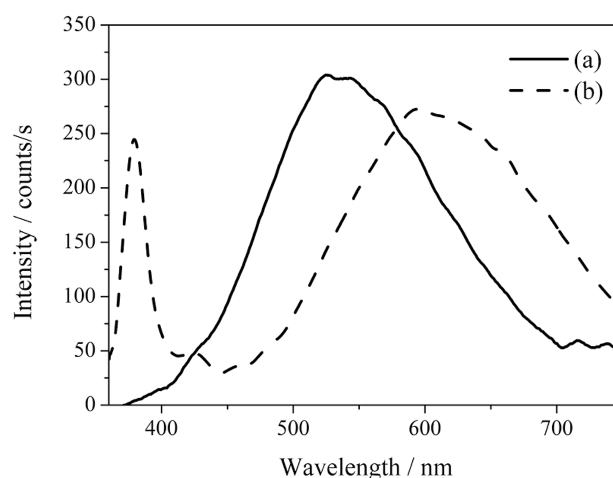

Fig.13. Photoluminescence spectrum of the ZnO thin film deposited from the DMSO solution on the silicon substrate with the buffer porous silicon layer at the current density 0.5 mA/cm^2 before (a) and after (b) hydrothermal ZnO deposition.

Fig.14 shows the photoluminescence spectra of ZnO crystals formed on the silicon substrate by the hydrothermal method in various temperature regimes. In these spectra, the intensive exciton photoluminescence band with maximum at the 380 nm wavelength may be distinguished. The photoluminescence band at 580 nm also is observed. The presence of this band is associated with the recombination processes via levels in the ZnO band gap created by ionized oxygen vacancies in accordance with mechanism discussed above [20]. The intensity increase of the photoluminescence bands for the samples formed at higher temperatures can be explained by the increase of total amount of semiconductor material grown on the substrate for the same time. However, it should be noted that the intensity of the ultraviolet band relative to the intensity of the yellow-green band increases as well with the temperature increase from 75°C to 85°C to be indicative of the crystal growth with higher crystal perfection. When the process temperature is increased up to 95°C, the intensity of the yellow-green band at 580 nm increases due to the increase in the oxygen defect concentration in the ZnO crystals.

click for feedback
consult - comment - contact
consult comment contact click for feedback

click for feedback
consult – comment – contact

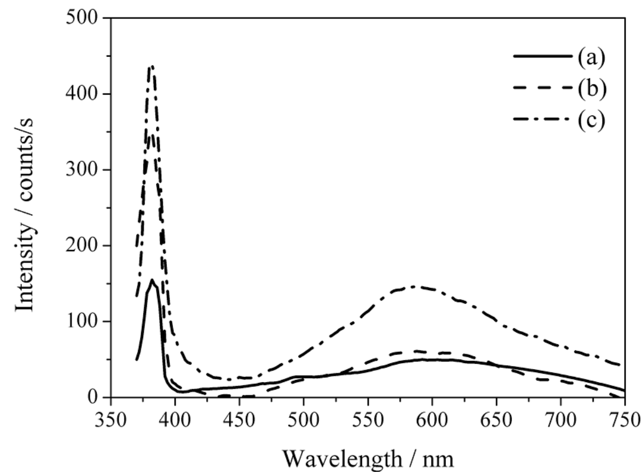

Fig.14. Photoluminescence spectra of ZnO crystals formed on the silicon substrate by the hydrothermal method at (a) 75°C, (b) 85°C, and (c) 95°C.

ZnO and Si integration and applications of ZnO/Si devices

The use of silicon substrates makes possible using commercial technological equipment for the large substrates, resulting in the reduction of manufacturing cost of the devices based on zinc oxide. Devices based on zinc oxide deposited on the silicon substrate may be made not only discrete, but may be integrated with the conventional silicon ICs either in the same package by the hybrid technology or in the same chip.

When zinc oxide base devices are integrated with the conventional silicon ICs within the same chip, a treatment of silicon wafer with zinc oxide regions already formed may be a considerable problem. Coefficients of thermal expansion of silicon and zinc oxide differ essentially (α_a = 6.51 $\mu m \cdot m^{-1} \cdot K^{-1}$ and α_c = 3.02 $\mu m \cdot m^{-1} \cdot K^{-1}$ for the different crystallographic orientations of ZnO and α = 2.6 $\mu m \cdot m^{-1} \cdot K^{-1}$ for Si) [22, 23]. Despite of buffer layers employed, the risk of the zinc oxide layer damage during high-temperature epitaxial and diffusion processes is very high. Hence, the zinc oxide deposition after the formation of active regions of silicon electronic devices, for example before the formation of metal interconnections, is seemed to be more advantageous. The low process temperature (< 100ºC) of the liquid methods of the zinc oxide deposition eliminates the risk of the damage of p-n junctions already formed in the silicon substrate. Zinc oxide may be deposited locally into the exposed regions of the masking layer. When the electrochemical deposition is used, an electric contact may be provided either from back side or front side of the substrate as illustrated in Fig. 15.

For the first case, a good ohmic contact should be provided to the back side of the substrate, and for the second case, special contact pads should be created on the front side. For the SOI substrates situation is more complex. BOX layer prevent current flow through whole substrate from bottom to top. To obtain electrical contact to the bulk Si substrate in certain areas BOX may be etched and in that case ZnO can be deposited in same manner as for bulk Si substrate, either using aluminum back side contact or with metal contact pad on top side. For the top side deposition BOX etching is not necessary. Metal contact pads may be formed directly on BOX.

For hydrothermal ZnO deposition electric contact is not needed but the strictly local zinc oxide deposition cannot be provided with this method. ZnO excess may be removed at further etching of the masking layer.

consult
comment
contact
click for feedback

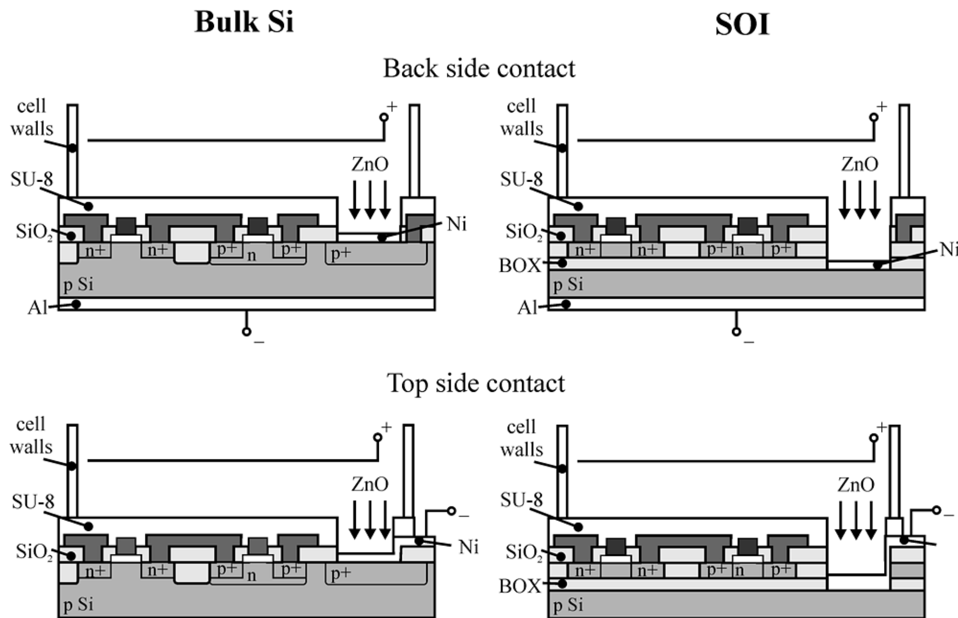

Fig.15 Variants of the ZnO electrochemical deposition on bulk silicon and SOI substrates with formed integrated circuits with electrical contact from the back side and from the top side.

Among possible applications of ZnO electrochemically deposited on bulk Si and SOI substrates we considered photodetectors, photovoltaic cells, humidity sensors, chemical gas sensors responding to hydrogen and gaseous hydrocarbons [24] and in piezoelectric devices [1]. Arrays of high-quality zinc oxide crystals with good photoluminescent properties formed by the hydrothermal method may be used in the light-emitting devices and nano-scaled piezoelectric energy generator [25]. High radiation hardness allows using ZnO based devices combined with a radiation hardened SOI circuitry in a harsh environment conditions.

Fig. 16 illustrates a construction of a silicon photodetector with a transparent conducting electrode made of electrochemically deposited zinc oxide and spectral sensitivity curve of the device. The photodetector consists of p-type silicon substrate with the porous silicon layer at the surface. The structure is conformally filled with zinc oxide which forms a continuous surface film. Spectral sensitivity broadening in the long-wave range of the electromagnetic spectrum with the energy less than silicon band gap energy is associated with the presence of levels in the band gap caused by surface defects in the porous silicon layer. Photovoltaic cell based on ZnO/Si structures works on the same principle.

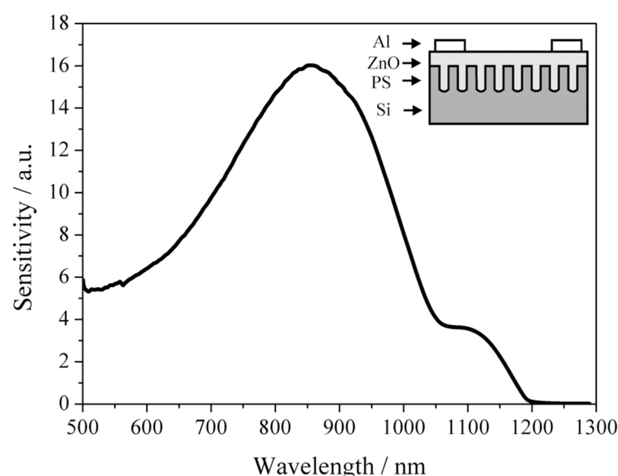

Fig.16. Spectral sensitivity of the photodetector based on the Si/PS/ZnO heterojunction.

Fig. 17 shows a construction and capacity vs. relative humidity plot for humidity sensor. Device consists of porous ZnO layer formed on the surface of the silicon substrate. On the top of the structure metal electrodes are placed. Capacitance of the structure strongly depends on relative humidity of the ambient air and varied in wider range than in case of conventional porous alumina based humidity sensors.

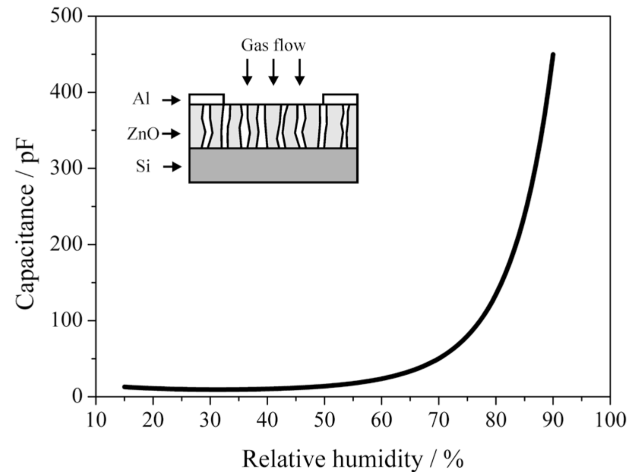

Fig.17. Responsibility of the humidity sensor based on the Si/ZnO structure.

Conclusions

Formation features of zinc oxide with various morphological structures deposited on the silicon substrates by liquid electrochemical and hydrothermal techniques are discussed in this work. By the electrochemical method, the zinc oxide films were formed on the silicon substrates with buffer porous silicon and porous silicon/nickel layers. When deposited on the metal buffer layer from the aqueous electrolyte, zinc oxide is formed as uniform continuous polycrystalline films consisted of crystallites with the preferred orientation (0002). When deposited on the porous silicon layer from the non-aqueous DMSO electrolyte, zinc oxide crystals were formed not only at the surface, but inside the porous layer as well. Arrays of zinc oxide crystals were deposited on the silicon substrates by the hydrothermal method. The crystals were of high crystal perfection and demonstrated high intensity of luminescence in the ultraviolet range. Photoluminescence spectra of the electrochemical zinc oxide films have one band corresponding to the defect levels in the ZnO band structure. Nevertheless, luminescence properties can be improved by hydrothermal deposition of ZnO crystals on electrochemical ZnO seed layer.

Aspects of ZnO electrochemical deposition on bulk silicon and SOI substrates for integration purposes were discussed. Examples of possible applications of ZnO/Si structures were also shown (photodetectors, humidity sensors)

Acknowledgements

The work has been supported by Belarus Government Research Program “Nanomaterials and nanotechnologies”, grant 6.12.03. Authors would like to thank V.Tzibulsky from “Belmicrosystems” for SEM study, A.Puskarev, L.Postnova and V.Levchenko from “Scientific-Practical Materials Research Centre of NAS of Belarus” SSPA for their help in XRD investigations, and V.Yakovtseva, L.Dolgyi, O.Kozlova and A.Yermalovich from Belarusian State University of Informatics and Radioelectronics for their help.

click for feedback
consult – comment – contact
consult
comment
contact
click for feedback

click for feedback
consult – comment – contact

References

[1] U. Ozgur, Ya.I. Alivov, C. Liu, A. Teke, M.A. Reshchikov, S. Doğan, V. Avrutin, S.-J. Cho and H. Morkoç: J. Appl. Phys. Vol. 98 (2005), p. 041301.

[2] Z.L.Wang: Materials Today Vol. 7 (2004), p. 26.

[3] D.C. Look, D.C. Reynolds, J.W. Hemsky, R.L. Jones and J.R. Sizelove: Appl. Phys. Lett. Vol. 75 (1999), p. 811.

[4] H. Ohta and H. Hosono: Materials Today Vol. 7 (2004), p. 42.

[5] J. Cembrero and D. Busquets-Mataix: Thin Solid Films Vol. 517 (2009), p. 2859.

[6] D. Lincot: Thin Solid Films Vol. 487 (2005), p. 40.

[7] S. Baruah and J. Dutta: Sci. Technol. Adv. Mater. Vol. 10 (2009), p. 013001.

[8] S. Hasegawa, K. Maehashi, H. Nakashima, T. Ito and A. Hiraki: J. Cryst. Growth Vol. 95 (1989), p. 113.

[9] V. Levchenko, L. Postnova, V. Bondarenko, N. Vorozov, V. Yakovtseva and L. Dolgyi: Thin Solid Films Vol. 348 (1999), p. 141.

[10] V. Yakovtseva, N. Vorozov, L. Dolgyi, V. Levchenko, L. Postnova, M. Balucani, V. Bondarenko, G. Lamedica, E. Ferrara and A. Ferrari: Phys. Status Solidi Vol. A 182 (2000), p. 195.

[11] E.B. Chubenko, A.A. Klyshko, V.A. Petrovich and V.P. Bondarenko: Thin Solid Films Vol. 517 (2009), p. 5981.

[12] V. Raiko, R. Spitzl, J. Engermann, V. Borisenko and V. Bondarenko: Diamond Relat. Mater. Vol. 5 (1996), p. 1063.

[13] E. Chubenko, V.P. Bondarenko and M. Balucani: Tech. Phys. Lett. Vol. B 60 (2009), p. 3320.

[14] S. Baruah and J. Dutta : J. Crystal Growth Vol. 311 (2009), p. 2549.

[15] M.N.R. Ashfold, R.P. Doherty, N.G. Ndifor-Angwafor, D.J. Riley and Y. Sun: Thin Solid Films Vol. 515 (2007), p. 8679.

[16] Ch. Liu, Y. Masud, Y. Wu and O. Takai: Thin Solid Films Vol. 503 (2006), p. 110.

[17] T. Yoshida, D. Komatsu, N. Shimokawa and H. Minoura: Thin Solid Films Vol. 451/452 (2004), p. 166.

[18] K.-H. Li, C. Tsai, S. Shih, T. Hsu, D.L. Kwong and J.C. Campbell: J. Appl. Phys. Vol. 72 (1992), p. 2816.

[19] D. Gal, G. Hodesa, D. Lincot and H.-W. Schock: Thin Solid Films Vol. 361/362 (2000), p. 79.

[20] W.C. Zhang, X.L. Wu, H.T. Chen, J. Zhu and G.S.Huang: J. Appl. Phys. Vol. 103 (2008), p. 3718.

[21] C. Mo, Y. Li, Y. Liu, Y. Zhang and L. Zhang: J. Appl. Phys. Vol. 83 (1998), p. 4389.

[22] J. Albertsson, S.C. Abrahams and A. Kvick: Acta Crystallogr., Sect. B: Struct. Sci. Vol. 45 (1989), p. 34.

[23] Y. Okada and Y. Tokumaru: J. Appl. Phys. Vol. 56 (1984), p. 314.

[24] S. Basu and P.K. Basu: Journal of Sensors Vol. 2009 (2009), p. 861968.

[25] Z.L. Wang: Adv. Funct. Mat. Vol. 18 (2008), p. 3553.

consult
comment
contact
click for feedback